



# Chemo-mechanical interactions between adsorbed molecules and thin elastic films

Matthew R. Begley<sup>a,b,\*</sup>, Marcel Utz<sup>c</sup>, Uday Komaragiri<sup>a</sup>

<sup>a</sup>*Structural and Solid Mechanics Program, Department of Civil Engineering, University of Virginia, Charlottesville, VA 22904, USA*

<sup>b</sup>*Department of Materials Science and Engineering, University of Virginia, Charlottesville, VA 22904, USA*

<sup>c</sup>*Department of Physics and Institute for Materials Science, University of Connecticut, Storrs, CT 06269, USA*

Received 21 October 2004; received in revised form 19 March 2005; accepted 21 March 2005

## Abstract

A general mechanics framework is presented to describe the interaction of molecular groups adsorbed on deformable thin films. Equations describing film deformation are expressed in terms of the pair potential that governs the interaction between adsorbed groups and large-deflection deformation descriptions. We illustrate that the pair potential can be used to define two-dimensional constitutive parameters for the adsorbed groups that describe their energetic contribution during arbitrary deformations. The framework is applicable to a wide range of interactions, including electrochemical interactions between a solution and film surface, interactions between neighboring adsorbed biopolymers and interactions between living cells. Key dimensionless parameters involving molecular interaction, surface coverage, film dimensions, and elastic properties are highlighted, and simplified governing equations for small deflections are identified. Solutions are presented that describe the influence of adsorbed groups on bending of cantilevers, pinned films and built-in (clamped) films. For clamped films, the critical molecular interaction parameters required to induce buckling are identified.

\*Corresponding author. Structural and Solid Mechanics Program, Department of Civil Engineering, University of Virginia, Charlottesville, VA 22904, USA. Tel.: +1 434 243 8728; fax: +1 434 982 2951.

E-mail address: [begley@virginia.edu](mailto:begley@virginia.edu) (M.R. Begley).

and post-buckling behavior discussed in terms of the implications for making biological sensors.

© 2005 Elsevier Ltd. All rights reserved.

*Keywords:* Adsorption; Films; Surface energy; Buckling

**1. Introduction**

Highly compliant structures such as thin films can deform substantially in response to interactions between molecules adsorbed on their surface. This phenomenon has been exploited to develop sensors to indicate the presence of adsorbed groups (e.g. Fritz et al., 2000; Moulin et al., 2000; Marie et al., 2002), to explore interactions between biological cells (e.g. Antonik et al., 1997), and to quantify surface stresses developed during electrochemical processes (e.g. Butt, 1996; Baller et al., 2000). Fig. 1 provides a schematic of the underlying concept for studies of interaction between adsorbed groups. Molecular binding sites are patterned on a flexible structure. If the binding sites are sufficiently close together, adjacent adsorbed groups interact, leading to noticeable deformation of the film. If the binding sites are selective, the structure acts as a chemically selective sensor whose deflection can be used to quantify the concentration of a particular molecular species.

The interaction between the adsorbate and the film is dictated by the ratio of the interaction energy between the adsorbed groups and the strain energy in the deformed film. The interaction energy between the surface molecules can arise from a wide number of mechanisms, including electrostatic repulsion, hydration forces (for adsorbed groups in solution), van der Waals forces (Israelachvili, 1992), and entropic interactions such as the repulsion between polymers end-grafted to the surface (Alexander, 1977; De Gennes, 1980; Milner, 1991; Hagan et al., 2002). In the following, the discussion is couched in terms of adsorbed molecules, although the

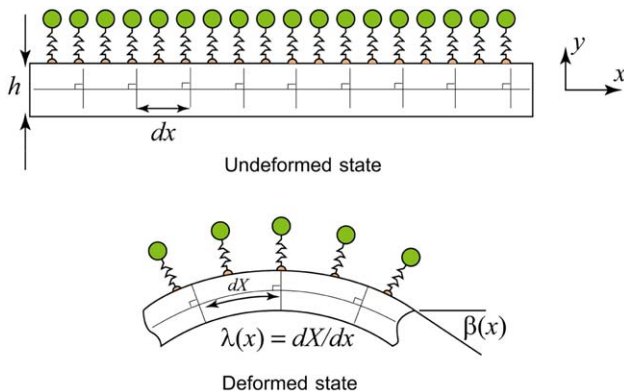


Fig. 1. Schematic illustration of adsorbed groups and elastic film with deformation variables.

framework is equally applicable to adsorbate interactions of any origin, including electrochemical processes that occur between a liquid and the film material itself (e.g. Butt, 1996).

For example, the deflection caused by single- and double-stranded DNA molecules end-grafted to the surface of  $\text{SiN}_x$  cantilevers has been calculated explicitly by Hagan et al. (2002), implying an isotropic deformation of the surface. The approach presented here separates the task of modeling the interaction between the adsorbed groups from that of solving the elasticity problem of the response of the micro-fabricated structure. This facilitates the treatment of more complex geometries, such as films subjected to plane strain conditions, films clamped at both ends, etc. In addition, it allows for the discussion of mechanical instabilities such as adsorption-induced buckling, which could be exploited to enhance sensitivity.

In general, the strength of interactions between adsorbed molecules on a surface can be expressed by a surface energy  $\gamma_0$ , which denotes the derivative of the total interaction energy with respect to a change in surface area at constant number of adsorbed particles (for a rigorous definition of  $\gamma_0$ , see Section 2.1). Similarly, the strain energy of the deformed beam can be considered in general terms as that arising from pure bending. As such, the fundamental physical quantity controlling the degree of interaction between the adsorbed groups and film is the coupling parameter:

$$A = \frac{\gamma_0 L^2}{Eh^3}, \quad (1)$$

where  $E$  is the elastic modulus of the film,  $L$  is the length of the film and  $h$  is its thickness.

When  $A \ll 1$ , the energy of surface interactions is small compared to that required to deform the beam, and coupling between the adsorbed groups and film deformation is negligible. Conversely, for sufficiently compliant film materials or thin films, the strain energy associated with bending may be comparable to the adsorbate interaction energy, and the mechanics of film deformation must include contributions arising from the presence of the adsorbed groups. The coupling parameter  $A$  clearly identifies scenarios where the surface (molecular) and film mechanics cannot be considered independently.

Previous works have demonstrated this coupling using ultra-thin films of relatively stiff materials. Butt (1996) illustrates that surface energies associated with a range of different types of surface interactions are in the range of  $1-30 \times 10^{-3} \text{ J/m}^2$ . For the case of a  $500 \mu\text{m}$  long polysilicon beam that is  $500 \text{ nm}$  thick; a surface energy change of  $5 \times 10^{-3} \text{ J/m}^2$  yields  $A \approx 1$ , indicating that interaction energy and strain energy are comparable. Compliant materials such as elastomers will lead to even stronger coupling (and more sensitive sensors); for a  $500 \mu\text{m}$  long *silicone* elastomer beam that is  $5 \mu\text{m}$  thick; an even smaller surface energy change of  $1 \times 10^{-6} \text{ J/m}^2$  yields  $A \approx 2$ . It is clear that, in principle, even stronger couplings are possible for lipid membranes, whose effective moduli and thickness can be much smaller than either of these examples (see for example, Israelachvili, 1992).

A general framework is presented to predict the effect of adsorbed groups on thin film deformation; the interaction energy is represented in terms of a pair interaction potential that depends on the distance between adsorbed groups, and is thus applicable to a wide range of interaction phenomena. Film deformation is described generally in terms of the large deformation of a linearly elastic material, with both bending and stretching effects included. The result is a set of governing equations that describes the deformed shape of the film in terms of the surface interaction potential, spatial distribution of adsorbed groups, and boundary conditions applied to the film.

An important application of the equations developed here is the behavior of films with fixed ends, which can experience out-of-plane buckling when group interactions are repulsive. This buckling instability offers an attractive pathway to develop ultra-sensitive sensors whose shape changes dramatically in the presence of adsorbates. Sensitivity can be greatly enhanced by designing films (i.e. with thickness and or residual stress) that are just beneath the bifurcation point prior to adsorption, such that small changes in surface conditions will trigger buckling. While the critical surface parameters needed to trigger buckling can be derived from a small-deflection analysis, the prediction of post-buckling displacements requires large-deflection kinematics. We illustrate that post-buckling displacements can be large enough to greatly improve sensor sensitivity, provided low-stiffness materials (such as glassy polymers or elastomers) are utilized.

## 2. Theoretical framework

### 2.1. Definitions of adsorption-, surface-, and surface interaction energies

In order to discuss the thermodynamics of adsorption, consider a system consisting of a solution with a certain fixed volume, in contact with a surface with a fixed number of binding sites. The change of free enthalpy upon addition of a solute molecule to the solution is given by

$$\Delta_S G = kT \ln \frac{\phi}{1 - \phi} + \mu_S^{\text{ex}}, \quad (2)$$

where  $\phi$  is the volume fraction of the solute. The  $1 - \phi$  term arises because at fixed volume, the addition of solute implies the removal of solvent. All non-ideal effects are accounted for in the excess chemical potential of solution,  $\mu_S^{\text{ex}}$ . Similarly, the change in free enthalpy upon adsorption of a molecule onto the surface is

$$\Delta_A G = kT \ln \frac{\sigma}{1 - \sigma} + \mu_A^{\text{ex}}, \quad (3)$$

where  $\sigma$  is the surface coverage (the fraction of binding sites that are occupied). The change in free enthalpy upon transition of a molecule from the solution to the

surface is given by the difference  $\Delta_A G - \Delta_S G$ :

$$\Delta_A G - \Delta_S G = kT \ln \frac{\sigma(1-\phi)}{(1-\sigma)\phi} + \Delta\mu_A^{\text{ex}}. \quad (4)$$

In thermal equilibrium, this quantity vanishes. This leads to a dependence of the surface coverage on the concentration with the excess free enthalpy of adsorption  $\Delta\mu_A^{\text{ex}} = \mu_A^{\text{ex}} - \mu_S^{\text{ex}}$  as a parameter. For  $\Delta\mu_A^{\text{ex}} = 0$ , we have the trivial case  $\sigma = \phi$ .

The excess free enthalpy of adsorption represents the non-ideal part of the change in free enthalpy upon transition of one molecule from the solution to the surface. We can write:

$$\Delta\mu_A^{\text{ex}} = \Delta\mu_B^{\text{ex}} + \Delta\mu_I^{\text{ex}}, \quad (5)$$

where  $\Delta\mu_B^{\text{ex}}$ , the excess chemical potential of binding, is independent of the surface coverage, and stems from the binding free enthalpy of an isolated molecule on the surface. The excess chemical potential of interaction,  $\Delta\mu_I^{\text{ex}}$  is due to interactions between adsorbed molecules, and depends on the interaction potential, the surface coverage, and the spatial distribution of adsorbed molecules. It is this contribution that we are concerned with in the following.

In thermodynamic equilibrium, the free enthalpy of adsorption is zero, since the chemical potentials of the molecules in solution and on the surface must be the same in this case. However, if the condition  $-\Delta\mu_A^{\text{ex}} \gg kT$  holds, a state of practically complete coverage is reached as soon as a (small) critical concentration is reached in the solution. In this case, slight changes in the chemical potential, induced by deformations of the surface discussed in the following, do not lead to noticeable changes in the surface coverage. It is this limit that is considered here.

Assume a surface homogeneously decorated with molecules at surface number density  $\rho$ . We further assume that the molecules interact through a pair potential  $\phi(r^2)$ . The excess free (Helmholtz) energy of interaction associated with a surface area of dimensions  $\pi r_0^2$  is then given as

$$F_I^{\text{ex}} = N \Delta\mu_I^{\text{ex}} = \rho\pi r_0^2 \int_0^{r_0} 2\pi\rho g(r)\phi(r^2)r dr, \quad (6)$$

where  $g(r)$  is the pair correlation function of the particles on the film, such that given a particle at the origin, the number of *other* particles in a surface area  $r dr d\theta$  is  $\rho g(r)r dr d\theta$ .

In the following, we are interested in changes in this energy upon stretching the film. The material points of attachment of the particles are assumed to remain the same in the deformation process. If the interaction between the adsorbed molecules is attractive, this leads to a line tension (or surface stress, with units  $\text{N/m} \equiv \text{J/m}^2$ ), providing resistance to an extension of the surface. For isotropic deformation, this “surface energy” is defined as

$$\gamma_0 = \left( \frac{\partial F_I^{\text{ex}}}{\partial A} \right)_{T,N} = -\rho^2 \left( \frac{\partial \Delta\mu_I^{\text{ex}}}{\partial \rho} \right)_T, \quad (7)$$

where Eq. (6) is transformed according to an radial expansion that corresponds to isotropic stretching of the film,<sup>1</sup> changing the interaction distance between particles. It is important to note that the derivative is taken at constant number of particles. This corresponds to the assumption that the change in surface area does not lead to adsorption or desorption, but only to a change in particle spacing.

The definition of the above energy is different from the surface tension of a liquid. In a liquid, the *density* of molecules in the surface remains constant. The surface tension is therefore defined as the derivative of the excess free enthalpy of the surface with respect to the area at constant density of the particles in the surface:

$$\gamma_L = \left( \frac{\partial F_S}{\partial A} \right)_{T,\rho} = \rho \Delta\mu_S, \quad (8)$$

where  $\Delta\mu_S$  is the difference in chemical potential of surface versus bulk molecules.

The surface energy of interaction  $\gamma_0$  is not identical to the surface energy of a solid as measured by a contact angle experiment. A subtle, but important, distinction must be made in the definition of the “surface tension” of a liquid and that of an elastic solid. For instance, when a soap bubble is inflated, the molecular structure of its surface does not change, and the surface interactions per unit area remain the same. The inflation therefore only increases the surface area of the bubble, but not the energy associated with the surface on a per-area basis. This leads to a resistance to inflation, called surface tension or surface energy. This surface energy provides the dominant contribution to the extensional stiffness of the soap bubble.

In a solid, the surface energy must be defined as the energy per unit area of new surface, created by cleaving a block of the material. This energy does not depend on the elastic strain of the material, since the same number of chemical bonds are broken to create the new surface irrespective of the elastic strain. Therefore, the surface energy, as measured by a contact angle experiment, does *not* usually make a contribution to the stiffness of an elastic solid body.

For this reason, it is misleading to attribute the adsorption-induced deformations of compliant elastic structures to a “change in surface energy”. Rather, the deformations are due to interactions between the adsorbed species, which are either attractive or repulsive depending on the spatial distribution of adsorbed groups and their interaction potential. Thus, we use the term “surface energy of interaction”, or simply interaction energy, to describe the energy associated with the interaction of adsorbed molecules on a surface.

## 2.2. Definition of the surface energy of interaction, or surface stress

Recall that Eq. (7) is defined for isotropic surface deformation, which leads to an isotropic surface energy of interaction, or surface stress. However, it is possible to consider non-uniform transformations of Eq. (6) and define a tensorial

<sup>1</sup>The energy associated with anisotropic deformations is considered in the next section.

representation for the surface stress, as in

$$\gamma_{ij} = \frac{1}{A} \frac{\partial F_1^{\text{ex}}(\epsilon_{ij}^S)}{\partial \epsilon_{ij}^S}, \quad (9)$$

where  $\epsilon_{ij}^S$  is a strain tensor that defines the transformation from the undeformed to the deformed geometry of the surface of the film. In this approach, the adsorbed molecules on the surface behave as a two-dimensional (2D) solid with the constitutive description:

$$\gamma_{ij} = \delta_{ij}(\gamma_0 + \lambda_0 \epsilon_{kk}^S) + 2\mu \epsilon_{ij}^S, \quad (10)$$

where the Lamé constants  $\lambda_0$  and  $\mu$  are properties of the *adsorbed* layer, and can be thought to represent an effective “stiffness” of the adsorbed groups. It has been assumed that the initial distribution of interacting groups is isotropic. These properties are defined in terms of the pair potential and pair correlation function of the adsorbed groups:

$$\gamma_0 = \frac{\pi\rho^2}{2} \int_0^\infty r^3 g(r) \phi'(r^2) dr, \quad (11a)$$

$$\lambda_0 = \frac{\pi\rho^2}{4} \int_0^\infty r^5 g(r) \phi''(r^2) dr, \quad (11b)$$

$$\mu = \frac{\pi\rho^2}{2} \int_0^\infty g(r) \left[ r^3 \phi'(r^2) + \frac{1}{2} r^5 \phi''(r^2) \right] dr. \quad (11c)$$

The primes denote derivatives with respect to the squared radial coordinate. The connection between Eqs. (6), (9) and (11a)–(11c) is described in Appendix A.

$\gamma_0$  represents the surface energy of interaction at zero film deformation, while  $\lambda_0$  and  $\mu$  represent contributions from the adsorbed groups arising during film deformation. Note that  $\gamma_0$  and  $\lambda_0$  can be either positive or negative, depending on whether the pair interaction is attractive or repulsive. The advantage of this approach is that the energetic contribution of the adsorbed groups can be described for arbitrary deformations (as opposed to purely isotropic deformation), using the same pair correlation function and interaction potential described above. Thus, one can derive the surface energy of interaction for plane strain deformations, as is considered below.

### 2.3. Kinematics of film deformation

A theoretical 2D framework is presented for arbitrary large film deformations where plane sections remain plane and perpendicular to the center-line of the film, as shown in Fig. 1. The restriction that plane sections remain plane implies that bending and stretch deformation in the film dominate shear deformation, but does not preclude large deformation. Deformation in the  $z$ -direction is assumed to be zero, such that only displacements in the  $x$ – $y$  plane must be considered.

The two kinematic variables describing the deformation of the film are the stretch ratio,  $\lambda(x)$ , and the rotation in the  $x$ - $y$  plane,  $\beta(x)$ . These are related to the displacements in the film as follows:

$$u'(x) = \lambda(x) \cos[\beta(x)] - 1, \quad (12)$$

where  $u(x)$  is the horizontal displacement of the film and the prime denotes differentiation with respect to the  $x$ -direction, and,

$$w'(x) = \lambda(x) \sin[\beta(x)], \quad (13)$$

where  $w(x)$  is the vertical displacement of the film. Thus, the formulation allows for large displacements that incorporate non-linear strain-displacement relationships.

Assuming that plane sections remain plane, but allowing for large displacements and stretch of the centerline, the total extensional strain distribution in the film in the deformed state is given by

$$\varepsilon_{xx}(x, y) = (\lambda(x) - 1) - \beta'(x)y, \quad (14)$$

where  $y$  is the distance from the deformed centerline of the film. Note that  $y = 0$  is not necessarily the neutral axis when adsorbed groups are present.

#### 2.4. Governing equations

For deformations confined to the  $x$ - $y$  plane, the internal virtual work (per unit width) done by a virtual increment in strain is given by

$$\delta W_{\text{int}} = \int_0^L \left[ \int_{-h/2}^{h/2} \sigma_{xx}(x, y) \delta \varepsilon_{xx}(x, y) dy \right] dx, \quad (15)$$

since  $\sigma_{yy} = \varepsilon_{zz} = 0$ . For a linearly elastic film subject to plane-strain conditions,  $\sigma_{xx} = \bar{E} \varepsilon_{xx}$ ; the plane-strain modulus is given by  $\bar{E} = E/(1 - \nu^2)$ , where  $E$  is the elastic modulus and  $\nu$  is the Poisson's ratio of the film. (Note that the present formulation can be easily modified to include non-linear constitutive descriptions for the film, i.e.  $\sigma = f(\lambda)$ .) The internal virtual work per unit width is then given by

$$\delta W_{\text{int}} = \int_0^L \{A(\lambda - 1)\delta\lambda + D(\beta')\delta\beta'\} dx, \quad (16)$$

where  $A \equiv \bar{E}h$  and  $D \equiv \bar{E}h^3/12$ .

As many applications involve a functional coating on the film, the means for calculating an effective modulus and effective thickness for a bi-layer is given in Appendix B; these quantities can then be simply substituted for the modulus and thickness in the following derivation. Note that the variation in stretch can be expressed in terms of the variation in axial displacements and rotations by taking the variation of Eq. (12):

$$\delta\lambda = \sec(\beta)\delta u' + (1 + u') \sec(\beta) \tan(\beta)\delta\beta. \quad (17)$$

This relationship is required if the boundary conditions for film deformation are expressed in terms of the vertical and horizontal displacements instead of stretch of the centerline and rotation.

The external virtual work per unit width (i.e. that attributed to the surface groups) due to an infinitesimal surface strain increment is defined through Eqs. (10) and (14):

$$\delta W_{\text{ext}} = \int_0^L \gamma_{xx} \delta \epsilon_{xx}^S dx = \int_0^L (\gamma_0 + E_G \epsilon_{xx}^S(x)) \delta \epsilon_{xx}^S(x) dx, \tag{18}$$

where  $E_G \equiv \lambda_0 + 2\mu$  is the effective plane-strain modulus of the adsorbed groups, and  $\epsilon_{xx}^S$  is the strain along the film surface, i.e.  $\epsilon_{xx}^S = \epsilon_{xx}(y = h/2)$ .

The governing equations can be found by applying the principle of virtual work.  $\delta W_{\text{tot}} = \delta W_{\text{int}} - \delta W_{\text{ext}} = 0$  implies:

$$\delta W_{\text{tot}} = \int_0^L [A(\lambda - 1)\delta\lambda + D(\beta')\delta\beta' - (\gamma_0 + E_G \epsilon_{xx}^S(x))\delta\epsilon_{xx}^S(x)] dx = 0. \tag{19}$$

It is convenient to normalize distances by the film length,  $L$ , and the total energy (per unit width) by  $\bar{E}hL$ . The results of this procedure are

$$\delta \hat{W}_{\text{tot}} \equiv \frac{\delta W}{\bar{E}hL} = \int_0^1 \left[ (\lambda - 1)\delta\lambda + \frac{\bar{h}^2}{12} \beta' \delta\beta' - (\Gamma_0 + \Sigma \epsilon_{xx}^S(x)) \delta \epsilon_{xx}^S(x) \right] d\bar{x} = 0, \tag{20}$$

where  $\bar{x} = x/L$ ,  $\bar{h} = h/L$ . The normalized surface energy of interaction and elastic modulus of the adsorbed groups are given by

$$\Gamma_0 = \frac{\gamma_0}{\bar{E}h}, \tag{21a}$$

$$\Sigma = \frac{E_G}{\bar{E}h} = \frac{\lambda_0 + 2\mu}{\bar{E}h}. \tag{21b}$$

After substituting Eq. (14) into Eq. (20), integrating by parts and collecting terms, one obtains the following governing equations:

$$\frac{d}{d\bar{x}} \left\{ \left[ \lambda(\bar{x}) - 1 + \Gamma_0 + \Sigma \left( \lambda(\bar{x}) - 1 - \frac{\bar{h}}{2} \beta'(\bar{x}) \right) \right] \sec \beta(\bar{x}) \right\} = 0 \tag{22}$$

and

$$\begin{aligned} \frac{d}{d\bar{x}} \left\{ \frac{\bar{h}^2}{12} \beta'(\bar{x}) - \frac{\bar{h}}{2} \left( \Gamma_0 + \Sigma \left( \lambda(\bar{x}) - 1 - \frac{h}{2} \beta'(\bar{x}) \right) \right) \right\} \\ - \left[ \lambda(\bar{x}) - 1 + \Gamma_0 + \Sigma \left( \lambda(\bar{x}) - 1 - \frac{\bar{h}}{2} \beta'(\bar{x}) \right) \right] \lambda(\bar{x}) \tan \beta(\bar{x}) = 0. \end{aligned} \tag{23}$$

This process also yields the following boundary conditions:

$$\left[ \lambda(\bar{x}) - 1 + \left( \Gamma_0 + \Sigma \left( \lambda(\bar{x}) - 1 - \frac{\bar{h}}{2} \beta'(\bar{x}) \right) \right) \right] \sec \beta(\bar{x}) \delta u(\bar{x}) \Big|_{0,1} = 0, \tag{24}$$

$$\left\{ \frac{\bar{h}^2}{12} \beta'(\bar{x}) - \frac{\bar{h}}{2} \left( \Gamma_0 + \Sigma \left( \lambda(\bar{x}) - 1 - \frac{\bar{h}}{2} \beta'(\bar{x}) \right) \right) \right\} \delta \beta(\bar{x}) \Big|_{0,1} = 0. \tag{25}$$

### 3. Linear solutions for small stretch and curvature

Displacements are normalized by the length of the film, i.e.  $\bar{u} = u/L$  and  $\bar{w} = w/L$ . For small deformations where  $\beta \ll 1$ ,  $\bar{h}\Sigma\beta' \ll 1$  and  $\bar{u}' \ll 1$ , and invoking Eqs. (12) and (17), the governing equations given as Eqs. (22) and (23) can be simplified to:

$$\bar{u}'' = 0, \tag{26}$$

$$(1 + 3\Sigma)\beta'' - \frac{12}{\bar{h}^2}(\Gamma_0 + (1 + \Sigma)\bar{u}')\beta = 0. \tag{27}$$

The boundary conditions given as Eqs. (24) and (25) become:

$$\left[ (1 + \Sigma)\bar{u}' - \frac{\bar{h}}{2}\Sigma\beta' + \Gamma_0 \right] \delta u \Big|_{0,1} = 0, \tag{28}$$

$$\left[ (1 + 3\Sigma)\frac{\bar{h}^2}{12}\beta' - \frac{\bar{h}}{2}(\Gamma_0 + \Sigma\bar{u}') \right] \delta \beta \Big|_{0,1} = 0. \tag{29}$$

The bracket terms in equations (28) and (29) are equivalent to the net axial force and moment applied to the film, respectively, derived from elementary beam theory.

#### 3.1. Cantilevered films with small deflections

For a cantilevered film, the variation at the right end is free, such that  $\delta\bar{u} = 0$  and  $\delta\beta = 0$ . This yields the following solution to Eqs. (26) and (27), subject to the boundary conditions implied by Eqs. (28) and (29):

$$\bar{u} = - \frac{\Gamma_0}{(1 + 4\Sigma)} \bar{x}, \tag{30}$$

$$\beta = \frac{6}{\bar{h}} \frac{\Gamma_0}{(1 + 4\Sigma)} \bar{x}. \tag{31}$$

The vertical displacements are then:

$$\bar{w} = \frac{3\Gamma_0}{\bar{h}} \frac{1}{(1 + 4\Sigma)} \bar{x}^2. \tag{32}$$

Note that for repulsive interactions,  $\Gamma_0 < 0$  and  $\Sigma > 0$ , such that the beam deflects away from the adsorbed groups. If the effective modulus of the adsorbed groups is zero (i.e.  $\Sigma \rightarrow 0$ ), one obtains the previously reported result (e.g. Butt, 1996):

$$w_{\max} = \frac{3\gamma_0 L^2}{\bar{E}h^2}. \tag{33}$$

### 3.2. Pinned films with small deflections

For geometries where both ends are fixed, the variation in displacement in the  $x$ -direction is zero, and the boundary conditions implied by Eq. (28) are automatically satisfied. The effects of pre-strain in the film can be accounted for by assuming the axial displacements are controlled by the fabrication process and are unchanged by the adsorption process. In this scenario, it is assumed that  $u'(x) \approx \varepsilon_0$ , where  $\varepsilon_0$  is a uniform pre-strain resulting from fabrication. This obviously satisfies Eq. (26). The solution to Eq. (27) is

$$\beta = C_1 \exp(\sqrt{\psi}\bar{x}) + C_2 \exp(-\sqrt{\psi}\bar{x}), \tag{34a}$$

where

$$\psi = \left(\frac{12}{\bar{h}^2}\right) \frac{(\Gamma_0 + (1 + \Sigma)\varepsilon_0)}{(1 + 3\Sigma)}. \tag{34b}$$

For *pinned* boundary conditions (i.e. rotations at the ends free), Eq. (29) implies the boundary conditions:

$$\beta'(0) = \beta'(1) = \frac{6(\Gamma_0 + \Sigma\varepsilon_0)}{\bar{h}(1 + 3\Sigma)}. \tag{35}$$

Enforcing these conditions yields the solution:

$$\beta = -\frac{6(\Gamma_0 + \Sigma\varepsilon_0)}{\sqrt{\psi}(1 + 3\Sigma)} \operatorname{sech}\left(\frac{\sqrt{\psi}}{2}\right) \sinh\left(\frac{\sqrt{\psi}}{2}(1 - 2\bar{x})\right). \tag{36}$$

Recall that Eq. (27) was derived assuming  $\beta \ll 1$ ,  $\bar{h}\beta' \ll 1$  and  $\bar{u}' \ll 1$ ; these assumptions imply this result should be interpreted in the limit that  $\Gamma_0 + (1 + \Sigma)\varepsilon_0 \ll 1$ , which yields:

$$\beta = \frac{6(\Gamma_0 + \Sigma\varepsilon_0)}{\bar{h}(1 + 3\Sigma)} \left(\bar{x} - \frac{1}{2}\right). \tag{37}$$

The displacement profile is thus:

$$\bar{w} = \frac{3(\Gamma_0 + \Sigma\varepsilon_0)}{\bar{h}(1 + 3\Sigma)} (\bar{x}^2 - \bar{x}). \tag{38}$$

Assuming the effective modulus of the adsorbed groups is zero, the maximum deflection of the film is

$$w_{\max} = -\frac{3\gamma_0 L^2}{4\bar{E}h^2}, \quad (39)$$

which is identical to the cantilever result if the length of the pinned–pinned beam is twice that of the cantilever. Note that in this case, for repulsive interactions ( $\gamma_0 < 0$ ) the film bows towards the side with the adsorbed groups.

### 3.3. Clamped films with small deflections

Assuming the displacements in the  $x$ -direction are controlled by pre-strain prior to adsorption (i.e.  $\bar{u}' = \varepsilon_0$ ), the solution to Eq. (27) is again given by Eq. (34a). For clamped films, the variation in displacement and rotations at the ends is zero, such that the boundary conditions given as Eqs. (28) and (29) are automatically satisfied. Hence, it is clear that the linearized forms of the governing equations cannot be used to solve for film deflection in the case of a clamped film. However, they can be used to identify the critical interaction energy that leads to buckling for cases where  $\Gamma_0 + (1 + \Sigma)\varepsilon_0 < 0$ . The condition  $\beta(0) = 0$  implies  $C_2 = -C_1$ ; the condition that  $\bar{w}(1) = 0$  implies:

$$\cos(\sqrt{\psi}) = \cos\left(\sqrt{\frac{12\Gamma_0 + (1 + \Sigma)\varepsilon_0}{\bar{h}^2(1 + 3\Sigma)}}\right) = 1. \quad (40)$$

Thus, the buckling criterion is given by

$$\frac{\Gamma_0 + (1 + \Sigma)\varepsilon_0}{(1 + 3\Sigma)} \leq -\frac{\pi^2 \bar{h}^2}{3}, \quad (41)$$

where the negative sign is a result of the fact that  $\Gamma_0 + (1 + \Sigma)\varepsilon_0$  must be less than zero for buckling to occur—otherwise the film is in tension. Neglecting the stiffness of the adsorbed groups, the critical interaction energy to induce buckling is

$$-\gamma_0^c = \bar{E}h \left[ 3.29 \left(\frac{h}{L}\right)^2 + \varepsilon_0 \right]. \quad (42)$$

Thus,  $\varepsilon_0 < 0$  corresponds to a compressive pre-strain that promotes buckling by lowering the absolute value of the critical interaction energy. In the limit that the interaction energy is zero, Eq. (41) implies the classical buckling result for a film subjected to a compressive pre-strain.

## 4. Non-linear solutions for large deformations and buckling displacements

Here, we present solutions for pinned and clamped films that experience large deflections. While the complete governing equations given by Eqs. (22) and (23) can be solved numerically with homogenous boundary conditions, simplified equations

can be developed for specific cases where interaction energy between adsorbed groups is small. Depending on the film geometry, this does not necessarily imply deformations will be small. Moreover, non-linear governing equations are needed to solve for post- buckling displacements. Here, the following assumptions are made:

$$\bar{u}' \equiv \varepsilon_0 \ll 1, \quad \bar{u}'' = 0, \quad \bar{h}\beta' \ll 1, \quad \Gamma_0 \ll 1, \quad \Sigma = 0. \quad (43)$$

None of these assumptions imply that the interaction parameter  $A$  given as Eq. (1) is small. Eq. (43) assume that the axial displacements are dominated by pre-stretch prior to adsorption. This is *not* equivalent to saying that stretching of the film is negligible; significant stretch can still be generated by large rotations. Eq. (43) assumes that changes in rotations are small over the length-scale defined by the film thickness; this is equivalent to saying that the separation of adsorbed groups is dominated by stretching of the film (as opposed to large curvatures, or “kinking” of the film). Again, the separation can still increase significantly from the initial state due to stretching caused by large rotations.

Eqs. (43) and (22) can be used to solve for the rotation gradient  $\beta'$  in terms of  $\beta$  and  $\beta''$ . This result is then used with Eq. (23) to yield:

$$\frac{\bar{h}^2}{12} \beta'' + \Gamma_0 \sin \beta + (1 - [1 + \varepsilon_0] \sec \beta) \sec \beta \tan \beta = 0. \quad (44)$$

The solution to Eq. (44) automatically satisfies both Eqs. (22) and (23), subject to the limitations of Eq. (43). In the limit of small rotations (i.e.  $\beta \ll 1$ ), Eq. (44) reduces to Eq. (27), as expected. According to the assumptions outlined above, Eqs. (12) and (13) imply the out-of-plane displacement is calculated using the solution to Eq. (44), using:

$$\bar{w}(\bar{x}) = \int_0^{\bar{x}} \tan(\beta(\hat{x})) d\hat{x}. \quad (45)$$

Solutions to Eq. (44) were generated using a finite-difference relaxation method that involves iteratively solving for rotations at discretized locations (e.g. [Press et al., 1992](#)). The method requires an initial guess for the rotation distribution, which will naturally depend on boundary conditions. Effective initial guesses are identified for pinned and clamped films in subsequent sections. Once a solution is obtained for specific values of  $\Gamma_0$  and  $\bar{h}$ , it can be used as the initial guess for slightly different values, leading to rapid convergence. Further details and examples of this numerical procedure are given by [Komaragiri et al. \(2005\)](#).

#### 4.1. Analytical solutions for the membrane limit with negligible bending stiffness

For sufficiently thin films or high interaction energies, the deformation will be large enough such that the films bending stiffness is negligible compared to that arising from stretching. Put another way, the present formulation encompasses both plate (linear) behavior and membrane (non-linear) behavior. In the membrane regime, the behavior independent of boundary conditions; bending influenced

regions are limited to a small boundary layer near the end-points, and do not significantly affect the maximum displacement.

With neglect of the bending (first) term in Eq. (44), one can solve directly for the resulting constant rotation (which is positive for  $\bar{x} < 1/2$  and negative for  $\bar{x} > 1/2$ ). Assuming small rotations and  $\Gamma_0, \varepsilon_0 \ll 1$ , which is clearly appropriate for the cases considered in subsequent sections, the behavior in the limit of zero bending is

$$\beta \cong \sqrt{2(\Gamma_0 - \varepsilon_0)} \tag{46}$$

which leads to the following prediction for maximum displacement:

$$\bar{w}_{\max} \cong \sqrt{\frac{(\Gamma_0 - \varepsilon_0)}{2}}. \tag{47}$$

The asymptotic behavior in the membrane regime is obviously independent of film thickness (save through the normalization of  $\Gamma_0$ ), since bending is negligible. Naturally, the  $\Gamma_0$  values for which bending can be neglected are a function of  $\bar{h}$ ; as the length of the film increases, one obtains the membrane limit at decreasing values of  $\Gamma_0$ . Note that the key assumption here is that  $\Gamma_0\beta \gg \bar{h}^2\beta''$ , which differs from the small angle limit used to derive the linear response for small  $\Gamma_0$ . Even though non-linear terms are important, rotations can still be small. The agreement between the numerical results discussed next and behavior for larger  $\Gamma_0$  values implies that the trigonometric functions in Eq. (44) can be accurately replaced with *non-linear* algebraic terms involving  $\beta$ .

#### 4.2. Results for pinned–pinned films

For a pinned film, the boundary conditions implied by Eq. (29) are:

$$\beta(0) = \beta(1) = \frac{6}{\bar{h}}(\Gamma_0 + \Sigma\varepsilon_0) \cos \beta. \tag{48}$$

The cosine term does not arise from a geometric effect concerning line tension acting at the end-points, but rather the decrease in repulsion due to non-linear stretching of the film at the end-points. (It turns out that for small values of  $\Gamma_0$ , the cosine term can be taken as unity.) For pinned films and small values of  $\Gamma_0$ , the linearized solution given as Eq. (37) can be used as the initial guess to find solutions in the non-linear regime.

Solutions to Eq. (44) are shown in Fig. 2, which depicts normalized maximum deflection versus  $\Gamma_0$  for a pinned film and several values of  $\bar{h} = h/L$  with  $\varepsilon_0 = 0$ . Both plate and membrane limits are immediately obvious; the plate limit is simply the small deflection result wherein  $w_{\max} \propto \Gamma_0$ . As  $\Gamma_0$  increases, bending effects become negligible and the behavior is that of a membrane, yielding  $w_{\max} \propto \sqrt{\Gamma_0}$ . The membrane result given as Eq. (47) is plotted in Fig. 2 along with the numerical results, and shows excellent agreement for larger values of  $\Gamma_0$ . Note that at large values of  $\Gamma_0$ , the results become independent of film thickness.

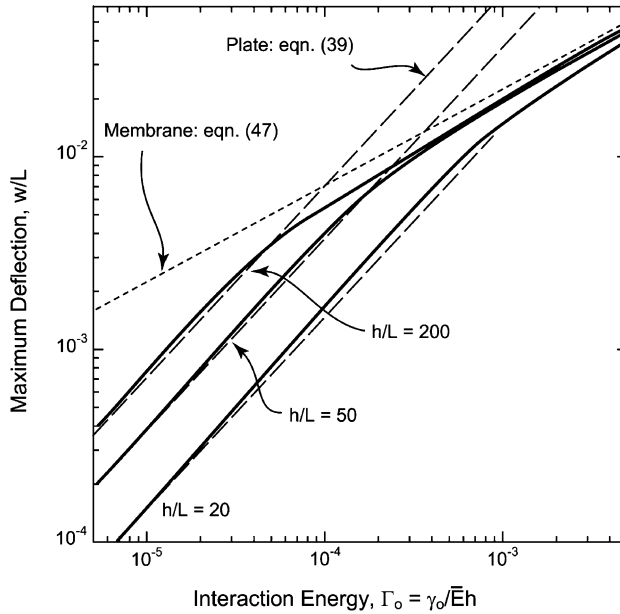


Fig. 2. Results for a pinned–pinned film without pre-strain.

### 4.3. Results for clamped films

For clamped films, the boundary conditions are  $\bar{w}(0) = \bar{w}(1) = \beta(0) = \beta(1) = 0$ . Beneath the critical buckling energy,  $\Gamma_0^c$ , the rotations are zero due to the fixed ends and the assumptions that  $\bar{u}' \equiv \varepsilon_0, \bar{u}'' = 0$ . (Put another way, the full governing equations are needed to allow out-of-plane displacements for energies beneath the buckling energy.) Above  $\Gamma_0^c$ , solutions to Eq. (44) can be found by starting with a large value of  $\Gamma_0$ , and using the membrane limit (Eq. (47)) as the initial guess.  $\Gamma_0$  is then decreased toward  $\Gamma_0^c$ , with previous solutions used as the initial guess. Using this approach, convergence of the relaxation method typically takes three to four iterations.

Fig. 3 illustrates the results for a clamped film and zero pre-strain, for several values of  $L/h = 1/\bar{h}$ . At the onset of buckling, out-of-plane displacements rise rapidly with increasing  $\Gamma_0$  and asymptotically approach the membrane solution. A key result is that thin films have small buckling energies, yet quickly can obtain displacements that are physically observable (note the normalization by film length). The presence of pre-strain (or residual stress) in the films changes the numerical values in Fig. 3, but not their qualitative appearance. That is, including pre-strain merely shifts the curves shown in Fig. 3. Compressive (negative) pre-strain lowers the buckling thresholds (as predicted by Eq. (41)), and increases the post-buckled displacements as predicted by the asymptotic membrane result (given as Eq. (47)). Conversely, tensile (positive) pre-strain will raise the buckling threshold and lower out-of-plane displacements.

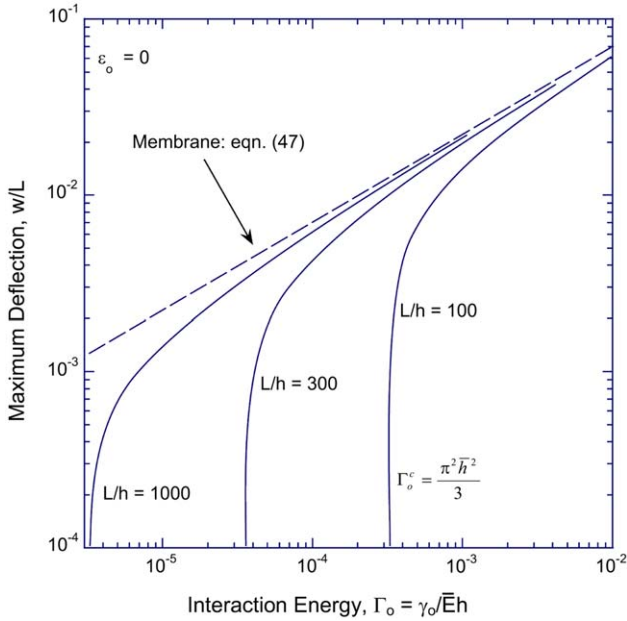


Fig. 3. Maximum out-of-plane displacements normalized by the film length vs. interaction energy, for a built-in film without pre-strain.

The results in Fig. 3 (and similar results involving pre-strain) can be collapsed onto a single curve by proper normalization. Fig. 4 plots the maximum out of plane displacement as function of the combined driving force for buckling,  $(\Gamma_0 - \varepsilon_0)$ , which is scaled by the critical value to induce buckling (see Eq. (41)). Results including pre-strain have not been included, as they fall directly on top of the results from Fig. 3 when this normalization is used. Obviously, the absolute value of interaction energy needed to induce buckling in Fig. 4 varies significantly with film length (since  $\Gamma_0^c$  scales with  $1/\bar{h}^2$ , as indicated by Fig. 3) and pre-strain (as indicated by the buckling criterion given as Eq. (41)). Displacements for  $|3(\Gamma_0 - \varepsilon_0)/\pi^2\bar{h}^2| > 1$  are essentially independent of film length for comparable changes in  $\Gamma_0 - \varepsilon_0$ . An important implication is that large displacements relative to the film thickness can be achieved at very small interaction energies.

A curve fit to the numerical results indicates that the following is a single global result that is accurate for  $100 \leq 1/\bar{h} \leq 1000$ :

$$\frac{w}{\bar{h}} \cong \left( \frac{3(\Gamma_0 - \varepsilon_0)}{\pi^2\bar{h}^2} - 1 \right)^{0.54}. \tag{49}$$

This result is within 5% of the numerical solutions for  $1.07 \leq 3(\Gamma_0 - \varepsilon_0)/\pi^2\bar{h}^2 \leq 100$ . Obviously, it is not asymptotically exact in the limit of large  $(\Gamma_0 - \varepsilon_0)$ , as the power-dependence is slightly different from the membrane solution. This fit is significantly more accurate over the range illustrated in Fig. 4.

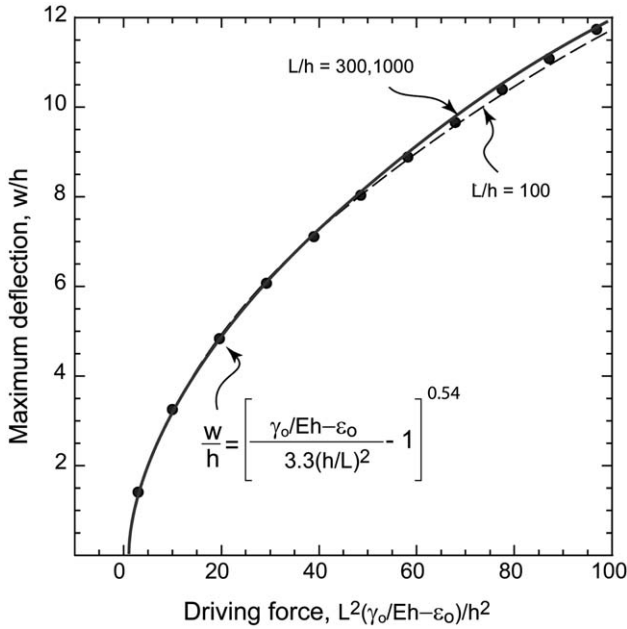


Fig. 4. Maximum out-of-plane displacement normalized by the film thickness vs. normalized driving force, for a built-in film without pre-strain.

### 5. Discussion

The illustrations presented in Sections 3 and 4 are most applicable to the development of sensors and assays designed to indicate the presence of adsorbed groups. With all dimensions being equal, the greatest sensitivity is obviously achieved using cantilevers while maximizing their length and minimizing their thickness. However, microfabrication of cantilevers can encounter significant obstacles as compliance is increased (i.e. by increasing their length or decreasing their thickness). Stiction failures become prevalent, and ceramic materials are prone to fracture.

Fabrication of built-in polymeric structures has several attractive advantages: (i) the dramatic reduction in modulus allows the same sensitivity to be achieved with larger spans and thicker films, (ii) using larger, built-in structures eases micro-fabrication challenges by enabling bench-top patterning and release procedures, and (iii) buckling behavior can be exploited to provide a discrete indicator of the presence of adsorbed groups. The central question is whether or not post-buckling displacements are large enough to observe experimentally for sufficiently small changes in surface energy.

Fig. 5 presents the displacement vs. surface energy change for several types of devices. For simplicity, it is assumed that pre-strain arising from fabrication is

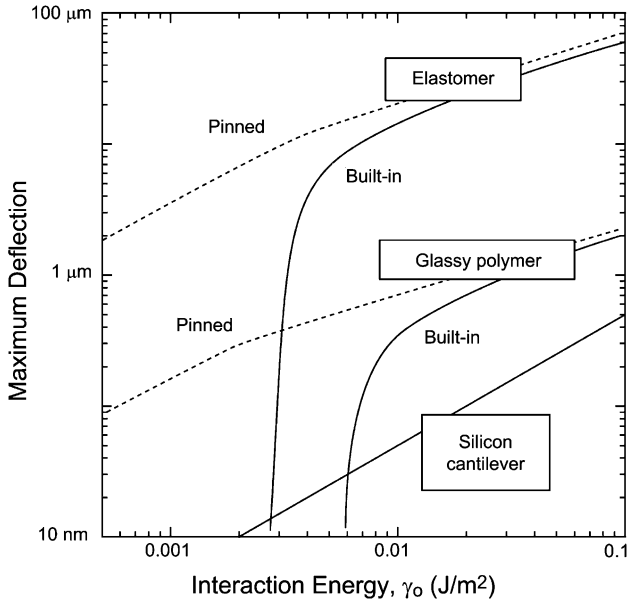


Fig. 5. Maximum out-of-plane displacement as a function of surface energy change, for several types of devices: *silicon cantilever*:  $h = 500$  nm,  $L = 500$   $\mu$ m,  $E = 200$  GPa, *glassy polymer, built-in* (e.g. PMMA):  $h = 500$  nm,  $L = 500$   $\mu$ m,  $E = 4$  GPa, *elastomer, built-in* (e.g. poly(dimethyl-siloxane, PDMS):  $h = 10$   $\mu$ m,  $L = 1000$   $\mu$ m,  $E = 1$  MPa.

negligible. The bottom straight line is a silicon cantilever with dimensions given in the figure caption. The two other sets of curves correspond to polymeric devices comprised of a glassy polymer and an elastomer. The dashed lines correspond to a pinned device, which would be difficult to fabricate: nevertheless, if the stiffness of the end points can be reduced (e.g. via focused ion beam milling), the reduced modulus of the polymer would more than make up for the pinning constraint, and far greater sensitivity is achieved over devices comprised of traditional semiconductor materials.

Built-in polymer films are easily generated via spin-casting and sacrificial etching of underlying layers (Maner et al., 2004). The examples shown in Fig. 5 demonstrate that dimensions can be tuned to generate buckling thresholds near the lower limit of displacement detection for cantilevers. Moreover, post-buckling displacements are then substantially larger—by orders of magnitude—than existing semi-conductor cantilever devices. In fact, for reasonable device dimensions, post-buckling displacements should be large enough to observe optically, eliminating the need for costly and sophisticated measurements involving lasers.

Naturally, the presence of pre-strain will strongly influence the performance of such devices, with two possibly detrimental effects. Positive (tensile) pre-strain will lower the sensitivity of the device (i.e. lower the output displacement for a given interaction energy) and may raise buckling thresholds beyond a useful limit.

Alternatively, negative (compressive) pre-strain may cause the films to buckle prior to group adsorption. The effectiveness of the normalization shown in Fig. 4 is a very useful result that allows one to quantify the effects of pre-strain. An important result is that the additional displacements due to surface adsorption on a *pre-buckled* structure (or pre-tensioned structure that still undergoes buckling) are specified by Eq. (49). Put another way, displacements arising from adsorption can be separated from those arising from pre-strain by suitable interpretation of Fig. 4.

It may be possible to adjust the pre-strain level via processing to tune the cantilevers to the onset of buckling, such that incredibly small changes in surface energy are readily detected. Moreover, in this approach, the out-of-plane displacements due to adsorption are significantly amplified by the presence of pre-strain, as post-buckling deformation occurs to relax the pre-strain in addition to the surface stress caused by adsorption. This strategy is most likely limited by thermal stability issues, as any thermal expansion mismatch between the film and supporting substrate also introduces pre-strain.

## 6. Concluding remarks

The present formulation is applicable not only to sensors designed to quantify surface interactions, but in the modeling of biological applications such as cellular interactions and membranes such as lipid vesicles. The framework presented here encompasses both bending and stretching, such that it may be applied to a wide range of film dimensions and ratios of surface energy and strain energy without a priori assumptions regarding their relative magnitudes. An important new result is the relationship between surface energy changes and film deformation in the buckling regime; the numerical results indicate that polymeric micro-devices that are accessible via existing micro-fab techniques will yield substantially larger displacements than existing micro-cantilevers.

## Acknowledgements

The authors are particularly indebted to Prof. J.G. Simmonds at UVA for many helpful mechanics discussions, particularly with regards to the non-linear buckling problem. MRB and MU gratefully acknowledge the financial support of the National Science Foundation through Grants CMS #9984517, and DMR #0094290, respectively.

## Appendix A. Elastic properties of a thin film

In the following, the elastic properties of a 2-D layer of adsorbed groups are derived from the pair interaction potential and the pair correlation function. The

generalized virial of a 2-D assembly of  $N$  particles is the second rank tensor:

$$V_{ij} = \sum_{k=1}^N r_{ki} f_{kj}, \quad \text{with } i, j = x, z \tag{A.1}$$

where  $\mathbf{r}_k = r_{ki}\mathbf{e}_i$  is the position vector of the  $k$ th particle and  $\mathbf{f}_k = f_{kj}\mathbf{e}_j$  the force acting on it. For particles interacting through a pair potential, the virial can be rewritten with a term representing the interaction with the external forces (stresses) and a double sum over the internal pair terms. Using elementary theorems of vector analysis, it can be shown that the external part of the virial is given by

$$V_{ij}^{\text{ext}} = A\gamma_{ij}, \tag{A.2}$$

where  $A$  is the surface area, and  $\gamma_{ij}$  represents the components of the 2-D stress tensor. The internal virial is given by the double sum:

$$V_{ij}^{\text{int}} = r_{lm,i} f_{lm,j} \tag{A.3}$$

with  $\mathbf{r}_{lm} = \mathbf{r}_l - \mathbf{r}_m$ . For a central pair potential, given by a function  $\phi(r^2)$ , the force of interaction between two particles is

$$\mathbf{f}_{lm} = - \frac{\partial \phi(\mathbf{r}_{lm}^2)}{\partial \mathbf{r}_{lm}}. \tag{A.4}$$

Obviously, this force is parallel to the separation vector. This makes it possible to write the internal part of the virial in terms of the (scalar) derivative of the interaction potential:

$$V_{ij}^{\text{int}} = -\phi'(\mathbf{r}_{lm}^2) r_{lm,i} r_{lm,j} \tag{A.5}$$

The generalized virial theorem states that  $V_{ij}^{\text{int}} + V_{ij}^{\text{ext}} = -2\delta_{ij}NK$ , where  $K$  is the kinetic energy per degree of freedom in the system. In the present case, we consider the particles to be fixed in their position, so the kinetic energy is zero by definition. Note that for a system of non-interacting particles, the internal virial is zero, and the external virial represents the pressure, whereas the kinetic energy is given by  $kT/2$ . The above equation then reduces to the ideal gas law.

The constitutive relation can be obtained by considering the dependence of the internal virial on the surface deformation tensor  $\varepsilon_{ij}^S$ . To first order in the strain, each particle pair makes a contribution to the internal virial given by:

$$V_{ij}^{\text{int}} = -\phi'(r^2)(r_i r_j + \varepsilon_{il}^S r_l r_j + r_i \varepsilon_{jl}^S r_l) - 2\phi''(r^2) r_l \varepsilon_{lm}^S r_m r_i r_j. \tag{A.6}$$

If the initial arrangement of the particles on the surface is isotropic, the internal virial can be found by integrating the above expression over the pair correlation function:

$$V_{ij}^{\text{int}} = - \frac{N\rho}{2} \int_0^\infty dr \int_0^{2\pi} r d\theta g(r) \left[ \phi'(r^2)r^2(c_i c_j + \varepsilon_{ik}^S c_k c_j + c_i \varepsilon_{jk}^S c_k) + 2\phi''(r^2)r^4 c_k \varepsilon_{kl}^S c_l c_i c_j \right], \tag{A.7}$$

where  $c_x = \cos \theta$  and  $c_z = \sin \theta$ . The angular integration is easily carried out. From the virial theorem, the surface stresses then emerge as

$$\gamma_{ij} = \delta_{ij}(\gamma_0 + \lambda e_{kk}^S) + 2\mu e_{ij}^S, \tag{A.8}$$

where  $\gamma_0$  is the (isotropic) surface stress at zero deformation, and  $\lambda, \mu$  are the planar elastic Lamé constants of the adsorbed layer. Eqs. (11a)–(11c) in the main text of the paper state these constants in terms of the pair potential and pair correlation function.

**Appendix B. Constitutive relationships for an elastic bi-layer**

For a bi-layer, an identical formulation can be used if the y-axis is defined relative to the neutral axis determined for pure bending. In this case, the distance from the bottom of the substrate to the neutral axis is given by

$$d = \frac{h_1^2 \bar{E}_1 + 2h_1 h_2 \bar{E}_2 + h_2^2 \bar{E}_2}{2(h_1 \bar{E}_1 + h_2 \bar{E}_2)}. \tag{B.1}$$

With appropriate change of the integration limits in Eq. (15), the film constants  $A$  and  $D$  (corresponding to stretching and bending stiffness, respectively) in Eq. (16) for a bi-layer are:

$$A_b = h_1 \bar{E}_1 (1 + \xi), \tag{B.2}$$

where  $\xi = h_2 \bar{E}_2 / h_1 \bar{E}_1$  and,

$$D_b = \frac{\bar{E}_1 h_1^3}{12} \left( \frac{1 + \xi [4 + (6 + \xi)(h_2/h_1)^2 + 4(h_2/h_1)^3]}{1 + \xi} \right). \tag{B.3}$$

The bi-layer can be replaced with an equivalent single film by defining an effective modulus and thickness such that the bending and stretching stiffness are identical to that of the bi-layer:

$$\bar{E}_e h_e = A_b \tag{B.4}$$

and

$$\frac{\bar{E}_e h_e^3}{12} = D_b. \tag{B.5}$$

Solving these two equations for the effective modulus and thickness, one obtains:

$$h_e = \sqrt{\frac{12D_b}{A_b}}, \quad \bar{E}_e = \sqrt{\frac{A_b^3}{12D_b}}. \tag{B.6}$$

These effective properties can be then used in the normalizations described in the main text to predict the response of the bi-layer. For a coating that is much thinner

than the substrate, i.e.  $h_2 \ll h_1$ , one obtains the following results:

$$h_e = h_1 \frac{\sqrt{1 + 4\zeta}}{(1 + \zeta)}, \quad \bar{E}_e = \bar{E}_1 \frac{(1 + \zeta)^2}{\sqrt{1 + 4\zeta}}. \quad (\text{B.7})$$

By way of illustration, consider a 10 nm thick gold coating ( $\bar{E}_2 \approx 90$  GPa) on a 10  $\mu\text{m}$  thick elastomer substrate ( $\bar{E}_1 \approx 1$  MPa): this yields  $\zeta \approx 9$ ,  $\bar{E}_e = 16.4$  MPa and  $h_e = 6.1$   $\mu\text{m}$ .

## References

- Alexander, S., 1977. Adsorption of chain molecules with a polar head. A scaling description. *J. Phys. (France)* 38, 983–987.
- Antonik, M.D., D'Costa, N.P., Hoh, J.H., 1997. A biosensor based on micromechanical interrogation of live cells. *IEEE Eng. Biol. Med.* 66–72.
- Baller, M.K., Lang, H.P., Fritz, J., Gerger, Ch., Gimzewski, J.K., Drechsler, U., Rothuizen, H., Despont, M., Vettiger, P., Battiston, F.M., Ramseyer, J.P., Fornaro, P., Meyer, H., Guntherodt, H.-J., 2000. A cantilever array-based artificial nose. *Ultramicroscopy* 82, 1–9.
- Butt, H.-J., 1996. A sensitive method to measure changes in the surface stress of solids. *J. Colloid Interface Sci.* 180, 251–260.
- Fritz, J., Baller, M.K., Lang, H.-P., Rothuizen, H., Vettiger, P., Meyer, E., Guntherodt, H.-J., Gerber, Ch., Gimzewski, J.K., 2000. Translating biomolecular recognition into nanomechanics. *Science* 14, 316–318.
- De Gennes, P.G., 1980. Conformations of polymers attached to an interface. *Macromolecules* 13, 1069–1075.
- Hagan, M.F., Majumdar, A., Chakraborty, A.K., 2002. Nanomechanical forces generated by surface grafted DNA. *J. Phys. Chem. B* 106, 10163–10173.
- Israelachvili, J., 1992. *Intermolecular and Surface Forces*. Academic Press, London, UK.
- Komaragiri, U., Begley, M.R., Simmonds, J.G., 2005. The mechanical response of freestanding circular elastic films under point and pressure loads. *J. Appl. Mech.* 72, 203–212.
- Maner, K.C., Begley, M.R., Oliver, W.C., 2004. Nano-mechanical testing of circular freestanding polymer films with sub-micron thickness. *Acta Mater.* 52, 5451–5460.
- Marie, R., Jensenius, H., Thaysen, J., Christensen, C.B., Boisen, B., 2002. Adsorption kinetics and mechanical properties of thiol-modified DNA-oligos on gold investigated by microcantilever sensors. *Ultramicroscopy* 91, 29–36.
- Milner, S.T., 1991. Polymer Brushes. *Science* 251, 905–914.
- Moulin, A.M., O'Shea, S.J., Welland, M.E., 2000. Micro-cantilever-based biosensors. *Ultramicroscopy* 82, 23–31.
- Press, W.H., Teukolsky, S.A., Vetterling, W.T., Flannery, B.P., 1992. *Numerical Recipes*. Cambridge University Press, Cambridge, UK.